

PCCP

Accepted Manuscript



This is an *Accepted Manuscript*, which has been through the Royal Society of Chemistry peer review process and has been accepted for publication.

Accepted Manuscripts are published online shortly after acceptance, before technical editing, formatting and proof reading. Using this free service, authors can make their results available to the community, in citable form, before we publish the edited article. We will replace this *Accepted Manuscript* with the edited and formatted *Advance Article* as soon as it is available.

You can find more information about *Accepted Manuscripts* in the [Information for Authors](#).

Please note that technical editing may introduce minor changes to the text and/or graphics, which may alter content. The journal's standard [Terms & Conditions](#) and the [Ethical guidelines](#) still apply. In no event shall the Royal Society of Chemistry be held responsible for any errors or omissions in this *Accepted Manuscript* or any consequences arising from the use of any information it contains.

Cite this: DOI: 10.1039/c0xx00000x

www.rsc.org/xxxxxx

ARTICLE TYPE

First-principles study of the sodium adsorption and diffusion on phosphorene

Xiao Liu,^a Yanwei Wen,^{*b} Zhengzheng Chen,^b Bin Shan^{b,c} and Rong Chen^{*a}

Received (in XXX, XXX) XthXXXXXXXXXX 20XX, Accepted Xth XXXXXXXXXXXX 20XX

DOI: 10.1039/b000000x

The structural, electronic, electrochemical as well as the diffusion properties of Na doped phosphorene have been investigated based on first-principles calculations. The strong binding energy between Na and phosphorene indicates that Na could be stabilized on the surface of phosphorene without clustering. By cooperating the Na atoms adsorption on one-side and both-sides of phosphorene, it is found the Na-Na exhibits strongly repulsion with the Na-Na distance less than 4.35 Å. The Na intercalation capacity is estimated to be 324 mAh/g and the calculated discharge curve indicates quite low Na⁺/Na voltage of phosphorene. Moreover, the diffusion energy barrier of Na atoms on phosphorene surface in both low and high Na concentrations are as low as 40–63 meV, which implies high mobility of Na during the charge/discharge process.

1. Introduction

Rechargeable solid-state batteries have joined in our daily life and been widely applied in portable electronics, electrical vehicles, and miscellaneous power devices.^{1–4} Due to the abundance of sodium (Na) and low redox potential (–2.71 V vs. standard hydrogen electrode),^{5,6} sodium-ion batteries (SIBs) have attracted much attention to relieve the urgent need of Li-ion batteries (LIBs), especially for large-scale energy storage. As a key component of SIBs, the anode materials are desired to be of high Na capacity, low redox potential, high electronic conductivity, high-rate Na diffusivity and robustly structural stability.⁷ Graphite, the commercial anode material for LIBs, is no more appropriate to encapsulate the Na effectively, due to the weak interaction between Na and the graphene plane, which affects the electrochemical performance.^{8–10} Other carbon-based structures (hard carbon, porous carbon), as well as porous and layered oxide materials (TiO₂, K_{0.8}Ti_{1.73}Li_{0.27}O₄, Na₂Ti₃O₇),^{11–16} are developed for SIB anode. However, the Na specific capacity of these materials is limited to 200 mAh/g. With high surface area and structural flexibility, two-dimensional (2D) material graphene is expected to be advantageous in SIB anodes. Although theoretical study implies that the binding between Na and pristine graphene is too weak for Na storage comparing with the cohesive energy of bulk Na, Datta *et al.* reveal that introducing defects in graphene could enhance the binding between Na and graphene and predict an enormous capacity (1450 mAh/g) in case of high defects concentration.¹⁷ Another theoretical work indicates that heteroatoms B doping into graphene could boost the Na storage capacity to 762 mAh/g.¹⁸ David *et al.* have experimentally fabricated the reduced graphene oxide (rGO) paper electrode, which exhibits the maximum

sodium charge capacity of ~140 mAh/g at 100mA/g.¹⁹ Another monolayer structure MoS₂, is investigated as potential candidate of SIB anode and the Na specific capacity is predicted to achieve as high as 335 mAh/g, which is larger than that of bulk MoS₂.^{20,21} Self-standing flexible electrode composed of few-layer MoS₂ and rGO flakes is prepared and shows a stable charge capacity of ~230 mAh/g with good Na cycling ability.²² However, the inferior carrier mobility of the monolayer MoS₂ limits its further application in SIB anode.

Elemental phosphorus (P) can form Na₃P compounds with a theoretical capacity of around 2600 mAh/g²³ and has attracted a lot of attentions from science community. Kim *et al.* have fabricated the red phosphorus/carbon composite which exhibits exceptional high Na storage capacity of about 1800 mAh/g.^{24–27} However, the over-all performance of these materials is still unsatisfactory mainly due to the low rate capacity which may be attributed to the low electronic conductivity and large volumetric expansion of red phosphorus. Recently, phosphorene, 2D monolayer black phosphorus, has been succeeded prepared by mechanical exfoliation method and exhibits promising electronic properties and high carrier mobility,^{28–30} which has been studied intensively for its potential application in electronics, optoelectronics, solar cell, photocatalyst and so on.^{31–35} Kulish *et al.* have investigated the adsorption of a series of metal atoms (Li, Na, K, Cu etc.) on phosphorene. They reported that the binding energy of alkali metal atoms to phosphorene is stronger than the cohesive energy of bulk structure, which implies the application of phosphorene on Li and Na storage.³⁶ A further theoretical study explores the Li doping properties on phosphorene³⁷ and predicts the Li capacity on monolayer phosphorene can reach 432 mAh/g, which is higher than that of commercial graphite materials. However, the Li diffusion barrier on phosphorene is as high as 0.76 eV, which may cause an inferior rate capacity when

phosphorene is used as LIB anode. Since it is reported that Na ions are faster than Li ions diffusing in the layered structures,^{38,39} phosphorene is expected to be more suitable to be used as the SIB anode. Up to now, the Na doping properties on phosphorene are still open and the evaluation of phosphorene as the SIB anode should be of great interest.

In this work, we have systemically studied the structural, electronic, electrochemical as well as the diffusion properties of Na doped phosphorene based on first-principles calculations. Our results show that the phosphorene is able to accommodate the Na atoms. The calculated band structures and density of states (DOS) suggest that the adsorption of Na can enhance the electronic conductivity of phosphorene. Na atoms adsorbed on one-side and both-side of phosphorene are systematically studied. It is found that the Na-Na interaction closely relates to the distance between Na atoms. A critical distance of about 4.35 Å for strong Na-Na repulsion is identified and the Na specific capacity can be estimated to be 324 mAh/g by a close packing of Na on the surface of phosphorene. The Na⁺/Na discharge curve related to the Na concentrations on phosphorene is simulated and several low and mild voltage plateaus are observed, which means a steady and high work voltage can be achieved when phosphorene is used as SIB anode. The diffusion barriers of Na atoms on phosphorene in both low and high Na concentrations are reported as 40~63 meV, which implies that it may possess outstanding rate capacity during charge/discharge process. Our calculations provide a comprehensive understanding of the interaction between Na and phosphorene.

2. Computational models and methods

All calculations are performed within density functional theory (DFT)^{40,41} framework by using the projector-augmented-wave (PAW)⁴² method, as implemented in the Vienna *ab initio* simulation package (VASP)⁴³⁻⁴⁵. The exchange and correlation energy was treated by generalized gradient approximation (GGA) with Perdew-Burke-Ernzerhof (PBE)⁴⁶ form. An energy cutoff of 400 eV is employed on the plane wave basis. The geometry optimization is performed till the Hellmann-Feynman force on each atom is smaller than 0.05 eV/Å. We adopt a 3 × 4 phosphorene supercell of 13.89 Å × 13.20 Å with a vacuum thickness of 15 Å to avoid the interaction between images slabs. The numerical integration in the first Brillouin zone is performed using a Monkhorst-Pack⁴⁷ grid of 5 × 5 × 1. To check the convergence, we have compared the total energy to the ones calculated with finer *k*-mesh and find the difference of total energy is smaller than 1 meV. A climbing image nudged elastic band (CI-NEB)⁴⁸ calculation is used to calculate the minimum energy path (MEP) of Na migration on phosphorene and to find the saddle point between two local minima for the system. Eight intermediate images are used for all CI-NEB calculations, which can map the MEP with reasonable accuracy.

3. Results and discussion

As shown in Fig. 1(a), different from pristine graphene, phosphorene is puckered with four P atoms in a unit cell (the red dash framework). The optimized lattice constants are 4.63 Å in *x* axis and 3.30 Å in *y* axis, which are in good agreement with

previous studies.^{49,50} The calculated P-P distances and ∠P-P-P angles in (P_A-P_B, ∠P_EP_AP_B) and out (P_B-P_C, ∠P_BP_CP_D) of the plane are 2.22 Å, 96.0° and 2.26 Å, 104.2°, respectively. Moreover, the first Brillouin zone and symmetric *k* points of the phosphorene supercell cell have also been presented in Fig. 1(a). According to the symmetry of phosphorene, there are four inequivalent sites for Na doping in the unit cell on one-side of phosphorene, which are labelled as *T* (on top of a P atom), *B* (on top of a P-P bond), *Br* (above the bridge site of two neighboring unbonded P atoms), *H* (above the hollow site of the triangular neighboring unbonded P atoms) in Fig. 1(a). Table 1 summarizes the calculated binding energies (*E_b*), the optimized bond lengths between Na and the nearest P (*d_{Na-P}*) and the charge transfer of adsorbed Na atom (Δ*Q*). The *E_b* is defined as:

$$E_b = E_{\text{phosphorene+Na}} - E_{\text{phosphorene}} - nE_{\text{Na,bcc}} \quad (1)$$

where, *E_{phosphorene+Na}*, *E_{phosphorene}* and *E_{Na,bcc}* are the total energies of Na-adsorbed phosphorene, pristine phosphorene and single Na atom in bulk structure (bcc), respectively. Therefore, the more negative of *E_b* means the stronger adsorption of Na on phosphorene compared with bulk structure. Note that the *d_{Na-P}* in all cases are about 2.80 Å, similar to previous reported distance of Na adsorbed on graphene and MoS₂.^{20,51} Among the four adsorption sites, the *H* site is the most favorable for Na with the *E_b* of -0.28 eV and the optimized structure of Na adsorbed on *H* site is presented in Fig. 1(b) (the other three adsorption configurations are presented in Fig. S1 in supporting information (SI)). The distances between the adsorbed Na atom and the nearest P atoms are 2.83 Å (*d₁*) and 2.92 Å (*d₂*), respectively. The negative binding energies of Na onto the *H* and *Br* sites reveal that Na atoms prefer to reside on the surface of phosphorene instead of clustering, suggesting that the phosphorene would be superior than graphene when used as SIB anode.^{17,18} The charge transfer between the Na atom and the phosphorene, Δ*Q*, is described by Bader charge analysis.⁵² The results in Table 1 show that the Na atoms adsorbed on *H* and *Br* site involve the larger charge transfer to phosphorene, which would be responsible for the stronger binding energy.

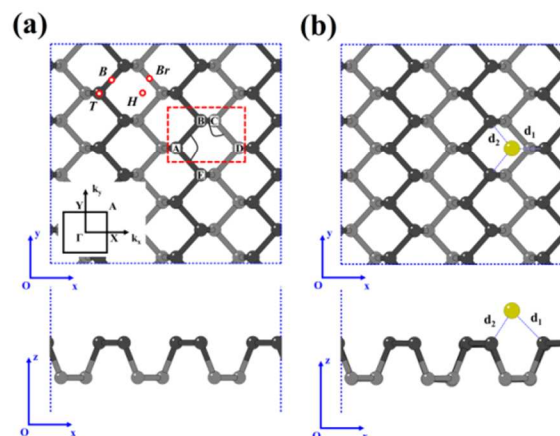


Fig.1 Top-view and side-view of (a) possible doping sites on pristine phosphorene, (b) single Na atom adsorbed on *H*-site of phosphorene. The phosphorus atoms in upper and bottom layers are highlighted by dark and light gray, respectively. The red dash square denotes the unit cell of phosphorene.

Table 1. Calculated binding energies (E_b), distances between Na and the nearest P of the optimized structures ($d_{\text{Na-P}}$) and the charge transfer of adsorbed Na atoms (ΔQ).

	<i>B</i>	<i>Br</i>	<i>H</i>	<i>T</i>
E_b (eV)	0.07	-0.24	-0.28	0.11
$d_{\text{Na-P}}$ (Å)	2.85	2.80	2.83	2.73
ΔQ (e)	0.81	0.83	0.83	0.80

Since the 2D monolayer phosphorene exhibits two sides of surfaces, we further explore the Na-Na interaction in the cases of one-side and both-side adsorptions on phosphorene. Fig. 2(a)-(d) illustrate that two Na atoms adsorbed on the same side, while (e)-(h) depict the two Na atoms adsorbed on the opposite sides individually. In each case, we have calculated E_b with different Na-Na distances. The optimized configurations ($d_{\text{Na-Na}}$), average binding energies ($\langle E_b \rangle$) as well as average charge transfer ($\langle \Delta Q \rangle$) per adsorbed Na atom are summarized in Fig. 2 and Table 2. To get a clear view of the binding energy and charge transfer to the Na-Na distance, they are plotted in Fig. 3(a) with the left and right parts denoting two Na atoms adsorbed on one-side and both-side of phosphorene. We notice the overall average binding energy per Na atom is slightly weaker than that of single adsorbed Na atom (red dash line) due to the Na-Na repulsion. In addition, $\langle E_b \rangle$ for both-side adsorption is stronger than that of one-side due to the weaker repulsion between the Na atoms in a larger distance. The important feature of Fig. 3(a) is that $\langle E_b \rangle$ of

one-side adsorption increases sharply when $d_{\text{Na-Na}}$ is shorter than 4.35 Å, which indicates the repulsion between neighboring Na atoms becomes drastically strong within the critical distance. It is interesting that the average charge transfer between Na and phosphorene follows a reverse trend with the binding energy, which is reasonable since the binding strength is mainly determined by the electronic interaction between them. It seems an exception for both-side adsorption that shorter Na-Na distance (6.4 Å) yields a lower binding energy, which is probably attributed to the screening effect of the phosphorene towards the Na-Na repulsion.

Table 2. Calculated distances between Na atoms of the optimized structures ($d_{\text{Na-Na}}$), average binding energies ($\langle E_b \rangle$), and average the charge transfer ($\langle \Delta Q \rangle$) of adsorbed Na atoms.

	$d_{\text{Na-Na}}$ (Å)	$\langle E_b \rangle$ (eV)	$\langle \Delta Q \rangle$ (e)
One-side adsorption	3.86	-0.15	0.74
	4.35	-0.22	0.78
	4.64	-0.23	0.79
	5.72	-0.23	0.81
Both-side adsorption	6.74	-0.29	0.80
	6.84	-0.28	0.80
	7.17	-0.26	0.81
	8.18	-0.25	0.82

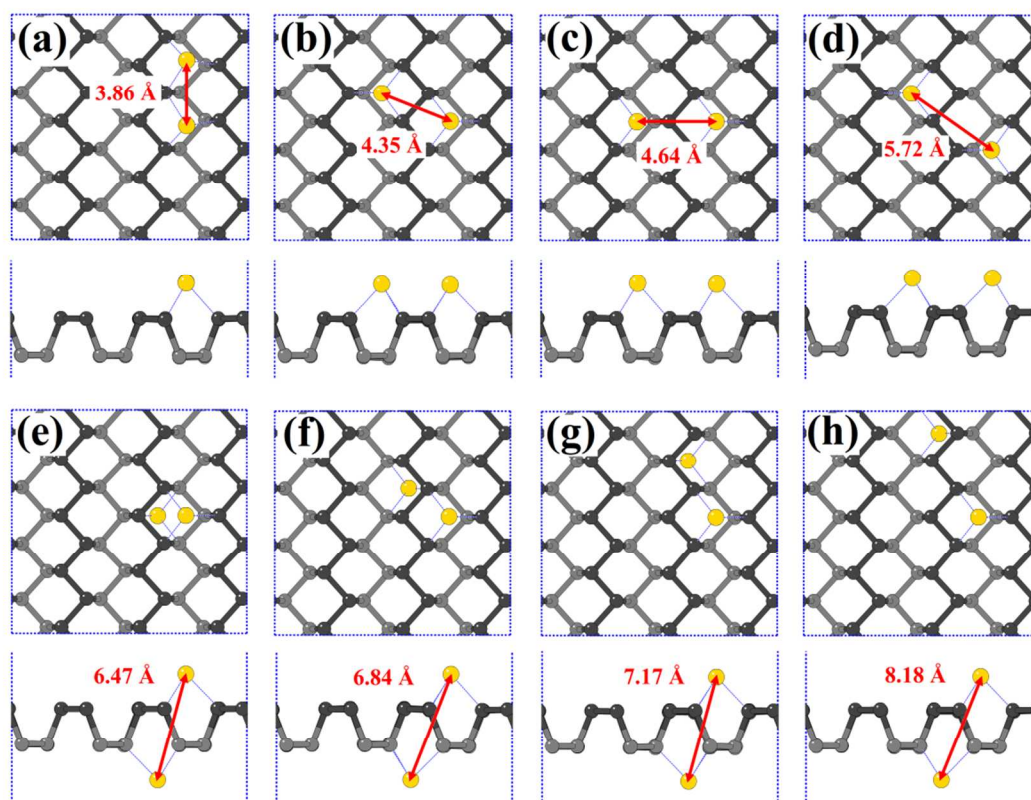


Fig.2 Top-view and side-view of two Na atoms adsorbed on (a)-(d) one-side and (e)-(h) both-side of phosphorene with different neighboring Na-Na distances.

40

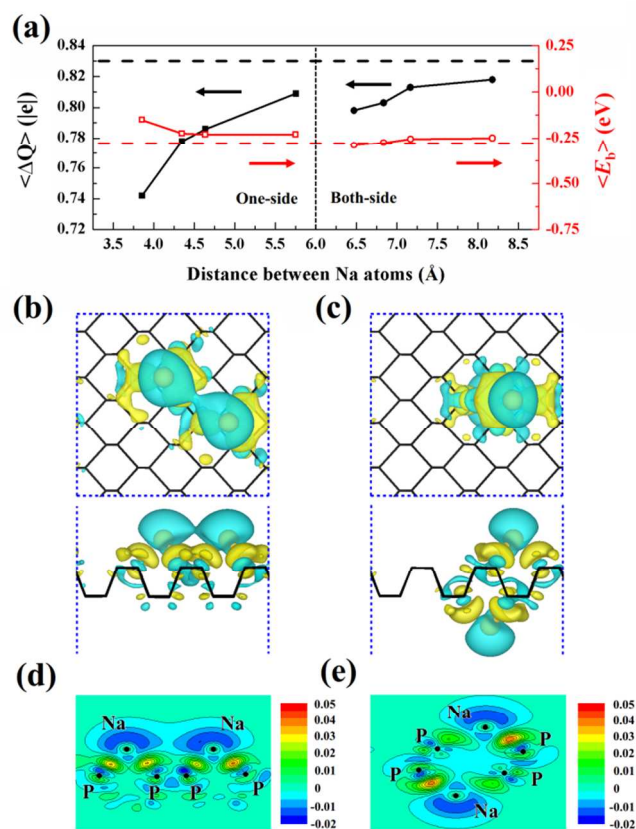


Fig.3 (a) Average binding energies ($\langle E_b \rangle$) and charge transfer ($\langle \Delta Q \rangle$) of two Na atoms adsorbed on phosphorene as a function of the Na-Na distance. The black and red dash lines represent the ΔQ and E_b of one Na adsorbed on phosphorene, respectively. (b) and (c) are the top and side views of the isosurface of the differential charge density of the structures shown in Fig. 2(d) and 2(e) with the increment level of $0.001a_0^{-3}$, where a_0 is the Bohr radius. The yellow and the grey-blue represent the positive and negative charge, respectively. (d) and (e) are corresponding contours of the differential charge density in side-views.

Fig. 3(b) and (c) show the isosurface of differential charge density ($\Delta\rho$) of two Na atoms on phosphorene with one-side (Fig. 2(d)) and both-side (Fig. 2(e)) adsorption, respectively. The $\Delta\rho$ is defined as:

$$\Delta\rho = \rho_{\text{phosphorene}+2\text{Na}} - \rho_{\text{phosphorene}} - \rho_{\text{Na-Na}} \quad (2)$$

where $\rho_{\text{phosphorene}+2\text{Na}}$, $\rho_{\text{phosphorene}}$ and $\rho_{\text{Na-Na}}$ are the charge densities of phosphorene with two adsorbed Na atoms, pristine phosphorene and an isolated Na dimer, respectively. There is obvious charge aggregation near the three nearest P atoms and charge dissipation around the Na-Na dimer, which indicates the formation of ion bonds between Na and phosphorene. The contours of $\Delta\rho$ for the two cases are shown from side-views in Fig. 3(d) and (e) to clarify this point. Since most charge of Na atoms are transferred to phosphorene, there should be repulsive interaction between the two Na ions in such a short distance. For the both-side adsorption, the negative charged phosphorene locates between the two Na ions and thus has a more effective screening effect compared to the case of one-side adsorption, where no screening medium exists between the two Na ions.

The band structure and density of states (DOS) have been calculated to investigate the electronic properties of phosphorene

by Na intercalation. The band structure and DOS of the pristine phosphorene are shown in Fig. 4(a) and it exhibits semiconducting behavior with a direct band gap of 0.94 eV, which agrees with the results of previous study.²⁹ Upon one Na atom doping, the change of the band structure follows a rigid band picture and the Fermi level upshift to cross the conductive band of phosphorene in Fig. 4(b), which implies a metallic behavior for the doped phosphorene. The partial density of state (PDOS) of Na atoms shows that the 2s electron of Na contributes the DOS near the Fermi level. The injection of 2s electron from the Na atom into the conduction bands of phosphorene pushes the Fermi level upward, which corresponds to the charge transfer as mentioned above. Fig. 4(c) shows the band structure and DOS of two Na atoms doped phosphorene with both-side adsorption. The change is similar with that of one Na atom adsorption. Additionally, the energy gap between the original conduction band minimum and valence band maximum of phosphorene decreases upon Na atoms doping, which may be attributed to the enhanced orbital hybridization between Na 2s and P 2p. Our band structure and DOS calculations indicate that the Na doping could promote the electronic conductivity of the phosphorene.

Since there are many equivalent H sites on both-side surface, it is expected that the phosphorene may exhibit high Na storage capacity. Knowing the critical distance for Na-Na strong repulsion is about 4.35 Å as discussed above, one can roughly estimate the upper limit of Na capacity. In order to avoid the strong interaction between Na atoms, each Na atom should exclusively occupy in an area of $4.35 \text{ \AA} \times 4.35 \text{ \AA}$, where there contains 4.95 P atoms. Thus the maximum Na concentration with both-side adsorption could reach $\text{Na}_2\text{P}_{4.95}$, corresponding to a theoretical capacity of 350 mAh/g since the capacity (C) can be calculate by:

$$C = \frac{\lambda F}{M_P} \quad (3)$$

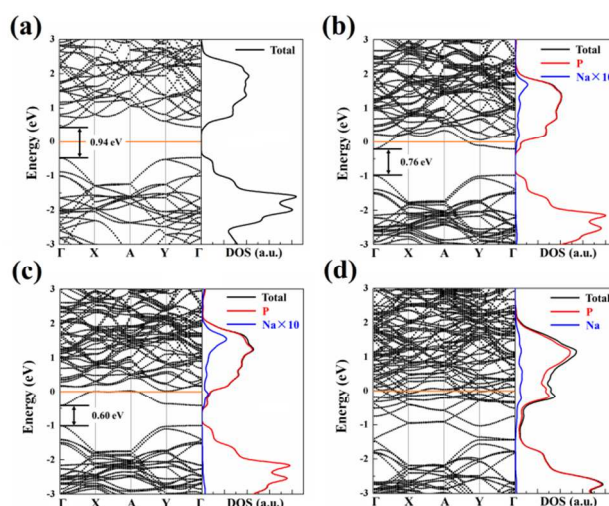


Fig.4 Band structure and DOS of (a) pristine, (b) one Na adsorbed, (c) two Na with both-side adsorbed and (d) 18 Na atoms adsorbed phosphorene. The total DOS, partial DOS (PDOS) of P and Na atoms are plotted with black, red and blue lines, respectively. Note that the PDOS of Na atoms in (b) and (c) have been scaled up ten times.

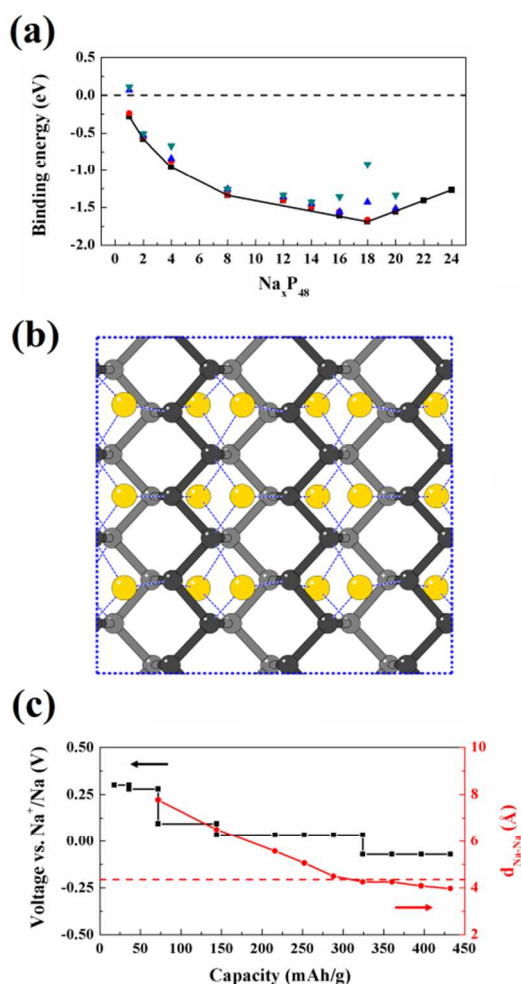
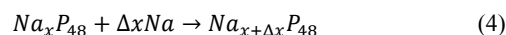


Fig.5 (a) Colorful symbols give the calculated Na binding energies of different configurations and constructed black line of convex hull indicates the ground states of phosphorene with different Na concentrations. (b) The most stable configurations of Na-doped phosphorene with formula of $\text{Na}_{18}\text{P}_{48}$. (c) Corresponding voltage profile and the average distance between neighboring Na atoms as a function of Na uptake. The red dash line represents the estimated critical distance of Na-Na strong repulsion.

where λ is the atomic ratio of Na and P atoms, F is the Faraday constant (26.8 Ah/mol), and M_p is the atomic mass of P (31g/mol). On the other hand, we calculate the binding energies of Na doped phosphorene with different concentrations ranging from Na_1P_{48} to $\text{Na}_{24}\text{P}_{48}$. For each concentration, several configurations (Fig. S2-S10 in SI) are considered to yield the most stable one. Fig. 5 shows all calculated binding energies and the hull line (the black solid line). The hull curve is a convex polyline within the whole range of the coverage, with its vertexes corresponding to all the true ground configurations of Na_xP_{48} . The total binding energy initially decreases with the increasing Na concentration and eventually saturates. Further Na intercalation would cause the weakening of the binding energy due to strong Na-Na repulsion. One should note that even with the highest Na stoichiometry $\text{Na}_{24}\text{P}_{48}$, in which all H site occupied by Na atoms on both sides of phosphorene (Fig. S10 in SI), the binding energy still is negative. However, its binding energy is about 0.41 eV less stable than the lowest point with formula of $\text{Na}_{18}\text{P}_{48}$ in Fig. 5(a) and the corresponding most stable configuration is shown in Fig. 5(b). Thus the largest Na

concentration corresponds to a capacity of 324 mAh/g, which agrees well with our above estimation. We further plot the band structure and DOS of $\text{Na}_{18}\text{P}_{48}$ in Fig. 4(d) and find the multiple Na atoms doping would increase the DOS of phosphorene near the Fermi level. The structural stability of the $p(2 \times 2)$ supercell of $\text{Na}_{18}\text{P}_{48}$ has also been considered during the charge/discharge processes by *ab initio* molecule dynamics simulation and the results show that the whole structure of phosphorene could be well-retained except for few atoms undergoing conversion-type reaction in some local region (Fig. S12 in SI). Moreover, the simulated result of fully discharged phosphorene with Na atoms removed can self-repair and be well recovered to the initial structure (Fig. S13 in SI).

The electrochemical properties of the phosphorene as SIB anode are investigated by Faraday laws. The discharge process can be described as Eq.(4), in which Δx indicates the number of intercalated Na atoms in each step:



The voltage given by Faraday laws is:

$$V(x) = \frac{-\Delta G}{e\Delta x} \quad (5)$$

where ΔG is the change of Gibbs free energy, which consists of three parts: $\Delta G = \Delta E + P\Delta V - T\Delta S$. In a solid-state reaction, $P\Delta V$ is in order of 10^{-5} eV and $T\Delta S$ is in order of the thermal energy (~ 0.026 eV). Thus ΔG can be well-approximated by the change of total energies (ΔE) obtained directly from first-principles calculations.⁵³ As shown in Fig. 5(c), there are two visible voltage plateaus during the discharge process. The first plateau is short with the Na^+/Na potential about 0.3 eV. The second one exhibits a relative low and wide range plateau, which implies a high and stable working voltage when used as SIB anode. The red curve in Fig. 5(c) presents the average distances between neighboring Na atoms with different Na concentrations. According to the most thermodynamically stable structure of compound $\text{Na}_{18}\text{P}_{48}$, the critical distance for strong Na-Na repulsion should be about 4.3 Å and is in good agreement with the result of two Na atoms adsorption.

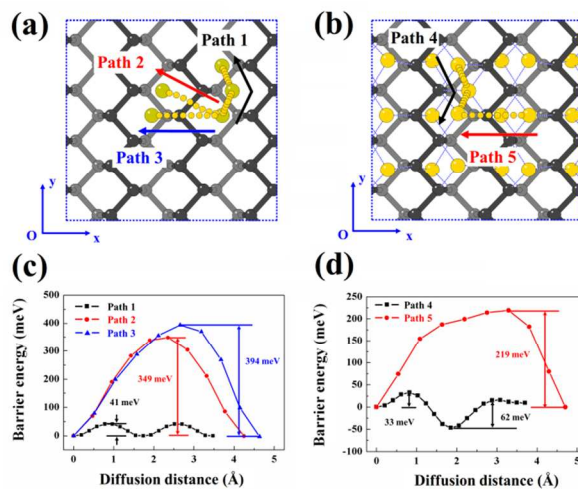


Fig.6 (a) and (c) are the possible diffusion paths and calculated minimum energy paths of Na on the surface of phosphorene for low Na concentrations, (b) and (d) are those diffusion paths and minimum energy paths for high Na concentrations.

Na-ion diffusion is an important factor affecting the rate capability of the SIBs. We focus on Na-ion diffusion on one-side of phosphorene plane. Fig. 6(a) shows three possible diffusion paths for Na according to the structural symmetry. Path 1 illustrates the Na migrating along the zigzag channel in y direction. In paths 2, Na-ion will cross over a protruding P-P bond to the neighboring channel normal to the y axis. Path 3 indicates a Na-ion migration over a protruding P atom to the neighboring channel aside path 2. The corresponding MEPs of Na diffusion in these three paths are shown in Fig. 6(c). Clearly, path 1 has the lowest energy barrier of 41 meV, only 1/8 and 1/10 that of path 2 and path 3. This indicates that Na ions mainly diffuse along in y direction. When the Na ion migrates between different channels, it would preferentially adopt path 2 by climbing over a P-P bond instead of a P atom since the latter exhibits a 50 meV higher energy barrier. The Na diffusion in high concentrations has also been considered. We chose the highest doping concentration $\text{Na}_{18}\text{P}_{48}$ as example and employ the model of $\text{Na}_{17}\text{P}_{48}$ where a Na vacancy is created to investigate the neighboring Na atoms migration. Two paths of Na diffusion along and across the channel are depicted as path 4 and path 5 in Fig. 6(b). The corresponding MEPs are calculated by CI-NEB and plotted in Fig. 6(d). The energy barriers for the two paths are also extremely low with barriers of 33 meV and 62 meV, respectively. It is interesting that the energy barrier of Na diffusion along path 5 is about half of that in path 1 when the Na atom migrates to another channel, which indicates the Na-Na repulsion benefits the Na diffusion in closely aligned patterns. We note that the Na diffusion barriers in both low and high concentrations are less than 70 meV, which is much lower than that of Li on phosphorene and Na on other reported 2D materials.^{18,20,37,54}

4. Conclusions

Based on first-principles calculations, we have systemically studied the adsorption and diffusion behaviors of Na on phosphorene. Our results indicate that phosphorene is able to accommodate the Na storage. By investigating the Na-Na interaction on phosphorene, a critical Na-Na repulsion distance is found and the Na intercalation capacity can be estimated to be 324 mAh/g. The calculated discharge curve of Na^+/Na reveals that phosphorene exhibits a stable voltage profile within a wide range. The diffusion energy barrier of Na on phosphorene is extremely low (~ 40 meV), which implies the phosphorene may exhibit outstanding rate capacity when used as SIB anode.

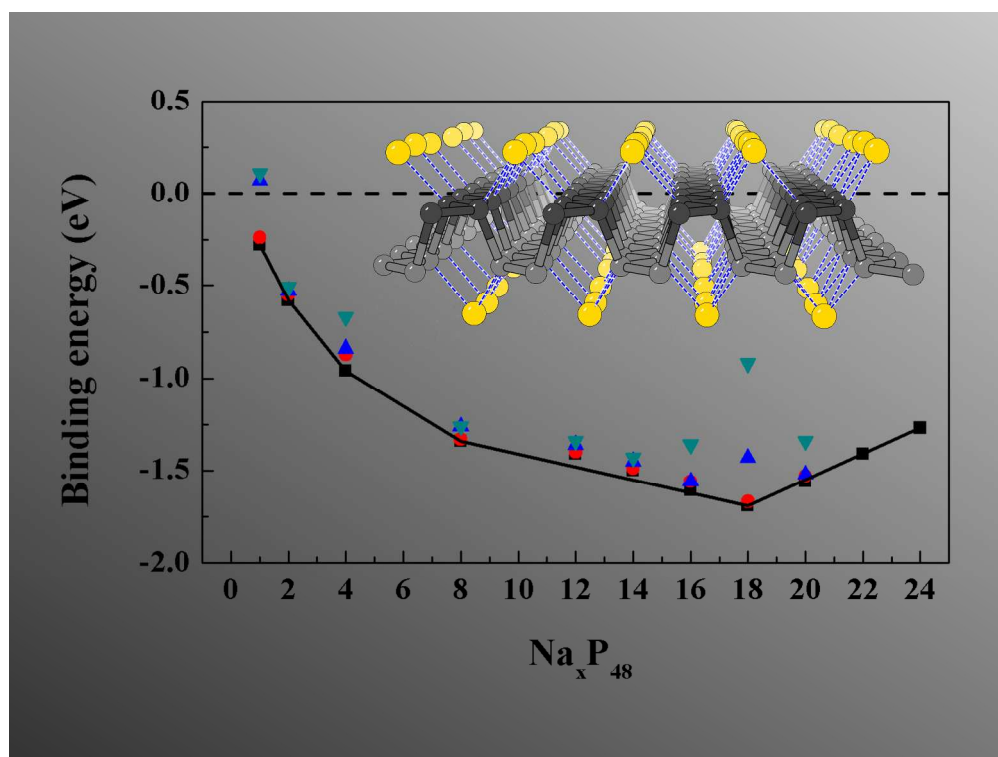
Acknowledgments

This work is supported by the National Basic Research Program of China (2013CB934800), National Natural Science Foundation of China (Grant 51302094 and 51101064), and the Hubei Province Funds for Distinguished Young Scientists (2014CFA018). Rong Chen acknowledges the Thousand Young Talents Plan the Recruitment Program of Global Experts and Changjiang Scholars and Innovative Research Team in University (No.: IRT13017). The calculations are done at the Texas Advanced Computing Center (TACC) at The University of Texas at Austin (<http://www.tacc.utexas.edu>).

Notes and references

- ^aState Key Laboratory of Digital Manufacturing Equipment and Technology and School of Mechanical Science and Engineering, Huazhong University of Science and Technology, Wuhan 430074, Hubei, People's Republic of China.
- ^bState Key Laboratory of Materials Processing and Die and Mould Technology and School of Materials Science and Engineering, Huazhong University of Science and Technology, Wuhan 430074, Hubei, People's Republic of China.
- ^cDepartment of Materials Science and Engineering, The University of Texas at Dallas, Richardson, Texas 75080, USA.
- † Electronic Supplementary Information (ESI) available: [configurations of Na doped phosphorene with different Na concentrations and the structural stability study of pristine phosphorene and $\text{Na}_{18}\text{P}_{48}$]. See DOI:10.1039/b000000x/
- * Corresponding author e-mail address: ywwen@mail.hust.edu.cn (Yanwei Wen); rongchen@mail.hust.edu.cn (Rong Chen).
- J. M. Tarascon and M. Armand, *Nature*, 2001, **414**, 359-367.
 - Y. W. Wen, X. Liu, X. B. Duan, K. Cho, R. Chen and B. Shan, *J. Phys. Chem. C*, 2013, **117**, 4951-4956.
 - M. Dahbi, N. Yabuuchi, K. Kubota, K. Tokiwa and S. Komaba, *Phys. Chem. Chem. Phys.*, 2014, **16**, 15007-15028.
 - J. Sun, G. Y. Zheng, H. W. Lee, N. Liu, H. T. Wang, H. B. Yao, W. S. Yang and Y. Cui, *Nano Lett.*, 2014, **14**, 4573-4580.
 - M. D. Slater, D. Kim, E. Lee and C. S. Johnson, *Adv. Funct. Mater.*, 2013, **23**, 947-958.
 - S. W. Kim, D. H. Seo, X. H. Ma, G. Ceder and K. Kang, *Adv. Energy Mater.*, 2012, **2**, 710-721.
 - X. F. Yu, G. Giorgi, H. Ushiyama and K. Yamashita, *Chem. Phys. Lett.*, 2014, **612**, 129-133.
 - D. P. DiVincenzo and E. J. Mele, *Phys. Rev. B*, 1985, **32**, 2538-2553.
 - D. A. Stevens and J. R. Dahn, *J. Electrochem. Soc.*, 2001, **148**, A803-A811.
 - S. Y. Hong, Y. Kim, Y. Park, A. Choi, N. Choi and K. T. Lee, *Energy Environ. Sci.*, 2013, **6**, 2067-2081.
 - R. Alcantara, J. M. Jimenez-Mateos, P. Lavela and J. L. Tirado, *Electrochem. Commun.*, 2001, **3**, 639-642.
 - K. L. Hong, L. Qie, R. Zeng, Z. Q. Yi, W. Zhang, D. Wang, W. Yin, C. Wu, Q. J. Fan, W. X. Zhang and Y. H. Huang, *J. Mater. Chem. A*, 2014, **2**, 12733-12738.
 - H. Xiong, M. D. Slater, M. Balasubramanian, C. S. Johnson and T. Rajh, *J. Phys. Chem. Lett.*, 2011, **2**, 2560-2565.
 - K. Y. Chen, W. X. Zhang, Y. Liu, H. P. Zhu, J. Duan, X. H. Xiang, L. H. Xue and Y. H. Huang, *Chem. Commun.*, 2015, **51**, 1608-1611.
 - J. Xu, C. Z. Ma, M. Balasubramanian and Y. S. Meng, *Chem. Commun.*, 2014, **50**, 12564-12567.
 - C. Deng, S. Zhang, Z. Dong and Y. Shang, *Nano Energy*, 2014, **4**, 81-87.
 - D. Datta, J. W. Li and V. B. Shenoy, *ACS Appl. Mater. Interfaces*, 2014, **6**, 1788-1795.
 - C. Ling and F. Mizuno, *Phys. Chem. Chem. Phys.*, 2014, **16**, 10419-10424.
 - L. David and G. Singh, *J. Phys. Chem. C*, 2014, **118**, 28401-28408.
 - J. C. Su, Y. Pei, Z. H. Yang and X. Y. Wang, *RSC Adv.*, 2014, **4**, 43183-43188.
 - M. Mortazavi, C. Wang, J. K. Deng, V. B. Shenoy and N. V. Medhekar, *J. Power Sources*, 2014, **268**, 279-286.
 - L. David, R. Bhandavat, and G. Singh, *ACS Nano*, 2014, **8**, 1759-1770.
 - N. Yabuuchi, Y. Matsuura, T. Ishikawa, S. Kuze, J. Y. Son, Y. T. Cui, H. Oji and S. Komaba, *ChemElectroChem*, 2014, **1**, 580-589.
 - Y. J. Kim, Y. W. Park, A. Choi, N. S. Choi, J. Kim, J. Lee, J. H. Ryu, S. M. Oh and K. T. Lee, *Adv. Mater.*, 2013, **25**, 3045-3049.
 - J. F. Qian, X. Y. Wu, Y. L. Cao, X. P. Ai and H. X. Yang, *Angew. Chem. Int. Ed.*, 2013, **52**, 4633-4636.
 - W. J. Li, S. L. Chou, J. Z. Wang, H. K. Liu and S. X. Dou, *Nano Lett.*, 2013, **13**, 5480-5484.

- 27 J. X. Song, H. X. Yu, M. L. Gordin, S. Hu, R. Yi, D. H. Tang, T. Walter, M. Regula, D. W. Choi, X. L. Li, A. Manivannan and D. H. Wang, *Nano Lett.*, 2014, **14**, 6329-6335.
- 28 L. Li, Y. Yu, G. J. Ye, Q. Ge, X. Ou, H. Wu, D. Feng, X. H. Chen and Y. Zhang, *Nat. Nanotechnol.*, 2014, **9**, 372-377.
- 29 H. Liu, A. T. Neal, Z. Zhu, Z. Luo, X. Xu, D. Tománek and P. D. Ye, *ACS Nano*, 2014, **8**, 4033-4041.
- 30 W. Lu, H. Nan, J. Hong, Y. Chen, C. Zhu, Z. Liang, X. Ma, Z. Ni, C. Jin and Z. Zhang, *Nano Res.*, 2014, **7**, 853-859.
- 31 J. S. Qiao, X. H. Kong, Z. X. Hu, F. Yang and W. Ji, *Nat. Commun.*, 2014, **5**, 4475.
- 32 V. Tran and L. Yang, *Phys. Rev. B*, 2014, **89**, 245407.
- 33 H. Y. Lv, W. J. Lu, D. F. Shao and Y. P. Sun, *Phys. Rev. B*, 2014, **90**, 085433.
- 34 J. Dai and X. C. Zeng, *J. Phys. Chem. Lett.*, 2014, **5**, 1289-1293.
- 35 B. S. Sa, Y. L. Li, J. S. Qi, R. Ahuja and Z. M. Sun, *J. Phys. Chem. C*, 2014, **118**, 26560-26568.
- 36 V. V. Kulish, O. I. Malyi, C. Persson and P. Wu, *Phys. Chem. Chem. Phys.*, 2015, **17**, 992-1000.
- 37 S. J. Zhao, W. Kang and J. M. Xue, *J. Mater. Chem. A*, 2014, **2**, 19046-19052.
- 38 S. P. Ong, V. L. Chevrier, G. Hautier, A. Jain, C. Moore, S. Kim, X. H. Ma and G. Ceder, *Energy Environ. Sci.*, 2011, **4**, 3680-3688.
- 39 R. Tripathi, S. M. Wood, M. S. Islam and L. F. Nazar, *Energy Environ. Sci.*, 2013, **6**, 2257-2264.
- 40 P. Hohenberg and W. Kohn, *Phys. Rev.*, 1964, **136**, B864-B871.
- 41 W. Kohn and L. J. Sham, *Phys. Rev.*, 1965, **140**, A1133-A1138.
- 42 G. Kresse and D. Joubert, *Phys. Rev. B*, 1999, **59**, 1758-1775.
- 43 G. Kresse and J. Hafner, *Phys. Rev. B*, 1993, **47**, 558-561.
- 44 G. Kresse and J. Hafner, *Phys. Rev. B*, 1994, **49**, 14251-14269.
- 45 G. Kresse and J. Hafner, *Comput. Mater. Sci.*, 1996, **6**, 15-50.
- 46 J. P. Perdew, K. Burke and M. Ernzerhof, *Phys. Rev. Lett.*, 1996, **77**, 3865-3868.
- 47 H. J. Monkhorst and J. D. Pack, *Phys. Rev. B*, 1976, **13**, 5188.
- 48 G. Henkelman and H. Jónsson, *J. Chem. Phys.*, 2000, **113**, 9978-9985.
- 49 Y. Li, S. X. Yang and J. B. Li, *J. Phys. Chem. C*, 2014, **118**, 23970-23976.
- 50 Z. Zhu and D. Tománek, *Phys. Rev. Lett.*, 2014, **112**, 176802.
- 51 Y. Wei and K. Manzhos, *MRS Commun.*, 2013, **3**, 171-175.
- 52 G. Henkelman, A. Arnaldsson and H. Jónsson, *Comput. Mater. Sci.*, 2006, **36**, 354-360.
- 53 M. K. Aydinol, A. F. Kohan and G. Ceder, *J. Power Sources*, 1997, **68**, 664-668.
- 54 V. V. Kulish, O. I. Malyi, M. F. Ng, Z. Chen, S. Manzhos and P. Wu, *Phys. Chem. Chem. Phys.*, 2014, **16**, 4260-4267.



The structural, electronic, electrochemical as well as the diffusive properties of Na doped phosphorene have been investigated, which indicates the phosphorene could be a promising sodium-ion battery anode based on first-principles study.
676x509mm (96 x 96 DPI)